VLBI polarization images of eight compact active galactic nuclei at $\lambda = 1.3 \text{ cm}$

D. C. Gabuzda 1,2* and T. V. Cawthorne³

¹Joint Institute for VLBI in Europe, Postbus 2, 7990 AA Dwingeloo, the Netherlands

Accepted 2000 July 11. Received 2000 June 19; in original form 2000 April 17

ABSTRACT

Global VLBI images in intensity and linear polarization at $\lambda=1.3\,\mathrm{cm}$ of the BL Lacertae objects 0235+164, 0300+470, 0735+178, 0954+658, 1803+784, 1823+568, and BL Lac and OVV quasar 3C 279 are presented and analysed. These are the highest resolution polarization images currently available for several of these sources. On the whole, the tendencies observed at longer centimetre wavelengths are also exhibited in these 1.3-cm images. When core polarization is detected, the corresponding polarization angles χ tend to lie either parallel or perpendicular to the direction of the inner jet. The core degrees of polarization are usually comparable to those typical at 6 cm, but somewhat lower in several cases, suggesting that the higher resolution data are better separating the contributions of intrinsically weakly polarized cores and highly polarized emerging knots. The observed χ vectors in the jets of 0735+178, 0954+658, 1823+568, BL Lac and 3C 279 are aligned with the jet, implying the presence of transverse magnetic fields. In 0300+470 and BL Lac, there are regions where the direction of χ seems to be neither parallel nor perpendicular to the jet; it is not clear whether this is due to genuine obliquity of the magnetic field structure or to inadequate knowledge of the local flow direction.

Key words: polarization – BL Lacertae objects: general – quasars: individual: 3C 279.

1 INTRODUCTION

BL Lacertae objects are active galactic nuclei whose most characteristic distinguishing property is their relatively low-luminosity optical line emission; frequently, their optical continua are completely featureless. Like many high-polarization quasars, BL Lacertae objects have strong and variable polarization in wavebands ranging from optical through radio; they usually have compact, flat-spectrum radio structure, and point-like optical structure. For some, luminous elliptical host galaxies are observed (Angel & Stockman 1980; Miller 1981; Kollgaard 1994), although the optical images of many BL Lacertae objects remain unresolved, even in high-resolution observations (e.g. Falomo 1996). The radio emission and much of the optical emission is believed to be synchrotron radiation.

Previous VLBI polarization observations of radio BL Lacertae objects at 3.6 and 6 cm (Gabuzda & Cawthorne 1996; Gabuzda et al. 1999, 2000 and references therein) revealed a tendency for the electric vector χ in polarized knots in the VLBI jets to be aligned with the local jet direction. The degrees of polarization in the jet components of BL Lacertae objects have been observed to

*E-mail: gabuzda@jive.nl

be as high as m = 60–70 per cent, with typical values m = 5–15 per cent, indicating that these components are optically thin and that in at least some cases the magnetic field is very highly ordered. This implies that the associated magnetic fields are perpendicular to the jet. One natural interpretation of this transverse magnetic field structure is that the visible jet components are associated with relativistic shocks that compress an initially tangled magnetic field, enhancing the magnetic field transverse to the compression (Laing 1980; Hughes, Aller & Aller 1989). Another possibility is that we are seeing the dominant toroidal component of helical fields associated with the jet (Gabuzda 1999; Gabuzda et al. 2000). It is clear that there are also a sizeable minority of BL Lacertae objects (about 30 per cent) in which, in contrast, longitudinal magnetic fields dominate in at least some parts of their VLBI jets.

At 6 cm, the degrees of polarization of the cores of BL Lacertae objects (2–9 per cent) are, on average, higher than those of quasars (\leq 2 per cent). Previous observations have shown the distribution of core χ orientations at 6 cm to be bimodal, with χ either aligned with or transverse to the inner jet direction (Gabuzda et al. 1994b, 2000).

It is of considerable interest to see if the characteristic polarization properties (i.e., magnetic field structures) displayed

²Astro Space Centre, Lebedev Physical Institute, 53 Leninsky Pr., 117924 Moscow, Russia

³Department of Physics and Astronomy, University of Central Lancashire, Preston, Lancashire PR1 2HE

in 3.6- and 6-cm global VLBI images are maintained on the scales probed by higher frequency VLBI observations. With this in mind, we obtained 1.3-cm polarization observations of seven BL Lacertae objects and the OVV quasar 3C 279 with the VLBA and the 100-m Effelsberg antenna. The resulting images show that the trends seen at lower frequencies are, for the most part, maintained on submilliarcsecond scales, although there is also evidence for more complex, possibly oblique magnetic-field structures in some sources.

2 OBSERVATIONS

The observations presented here were made in 1995 July (1995.58), using an 11-element global VLBI array consisting of the US VLBA and the 100-m Effelsberg antenna. The antennas used are listed in Table 1. The VLBA antennas recorded both right and left circular polarization (RCP and LCP), while Effelsberg recorded only LCP. The data were recorded at a total rate of 128 Mbits s⁻¹ with two-bit sampling, in four 8-MHz baseband converters per polarization. The data were correlated at the VLBA correlator in Socorro, New Mexico.

We calibrated the data in the NRAO AIPS package using standard techniques. The solution for the instrumental polarizations (D-terms) was based on eight scans for the unpolarized source 3C 84 covering a large range of parallactic angles.

The most common method used to calibrate the absolute orientation of the polarization position angles χ is to compare the total polarization of a compact polarized source on VLBI scales with simultaneous or nearly simultaneous integrated polarization measurements for this source; we then find the rotation required to make the VLBI and integrated χ values agree. However, no integrated measurements at 1.3 cm were available near the time of our observations. We therefore gathered the integrated 2-cm data from the data base maintained by the University of Michigan Radio Astronomy Observatory that were nearest to our VLBI observations for all our programme sources. Inspection of the 2-cm Michigan polarizations suggested that the sources 3C 279 and 1823+568 had large polarized fluxes and relatively stable integrated χ values near the epoch of the VLBI observations, making them best suited as polarization position angle calibrators. Comparison of the 2-cm Michigan and 1.3-cm short-baseline VLBI polarizations for 3C 279 and 1823+568 demonstrated that a large fraction of the integrated polarized flux was present on VLBI scales, and yielded χ offsets for the two sources that were in agreement to within 5°. We adopted the average of these offsets to calibrate the polarization position angles for all the sources. Despite potential inaccuracy due to the (small) wavelength

Table 1. Antennas used.

Antenna	Diameter (m)	T _{sys,R} (K)	T _{sys,L} (K)	(K Jy ⁻¹)
Effelsberg, Germany	100	-	140	0.793
St. Croix	25	205	215	0.107
Hancock	25	120	115	0.092
North Liberty	25	135	140	0.108
Fort Davis	25	120	100	0.095
Los Alamos	25	105	125	0.102
Pietown	25	115	115	0.130
Kitt Peak	25	100	100	0.115
Owens Valley	25	110	110	0.088
Brewster	25	120	120	0.099
Mauna Kea	25	75	90	0.106

difference between the integrated and VLBI data, and to the fact that the integrated and VLBI polarization measurements were not simultaneous, the good consistency in the results yielded by the two independent sources leads us to believe that the resulting χ values are accurate to within about 5°.

Maps of the distribution of total intensity I were made in the AIPS package using the tasks CALIB and IMAGR. During the imaging process, the RL and LR ('cross-hand') data were calibrated using the antenna gains determined using the corresponding RR and LL data. Maps of the linear polarization P were then made by Fourier-transforming the cross-hand fringes and performing a complex CLEAN using the AIPS procedure CXPOLN and the task CXCLN. This procedure was necessary since the Effelsberg antenna recorded only LCP, so that the resultant cross-hand u-v coverage was not symmetrical. Since the same antenna gains were used to calibrate all four correlations, the resulting I and P maps are registered to within a small fraction of a beamwidth, so that the corresponding images can be directly compared.

3 RESULTS

In each of the VLBI images presented here (Figs 1–8), the restoring beam is shown as an ellipse in a corner of the image. The restoring beams are typically $0.5 \times 0.3 \,\mathrm{mas^2}$. For the linear polarization maps, the contours are those of polarized intensity p, and the plane of the electric vector is indicated by the polarization position angle vectors that are superimposed.

There is always the possibility that the observed VLBI polarization position angles include some contribution due to Faraday rotation along the line of sight to the emission region. The largest integrated rotation measure is that for BL Lac, RM = $-205 \, \mathrm{rad} \, \mathrm{m}^{-2}$, which corresponds to a rotation of only $\simeq 2^{\circ}$ at 1.3 cm. It is therefore clear that the effect of the Galactic component of the source rotation measures will be negligible in the images presented here, and we have made no correction for this component.

There is solid evidence for the presence of enhanced rotation measures in the core regions of a number of quasars, including 3C 279 (Taylor 1998), which reach values large enough to imply appreciable rotations at 1.3 cm; we will discuss this in more detail below in connection with our P image of 3C 279. Little information is available about the distribution of local Faraday rotation in the immediate vicinities of the VLBI structures of BL Lacertae objects. There is some evidence that the parsec-scale rotation-measure distribution of 1803+784 is non-uniform (Gabuzda 2000), but the maximum estimated rotation measures are far too small to imply appreciable rotations at 1.3 cm. A region of enhanced rotation measure has been detected in the VLBI jet of 0820+225 (Gabuzda et al., 2001), but there, also, the maximum rotation measure is only a few hundred rad m⁻², which is too small to give more than a $2^{\circ}-3^{\circ}$ of rotation at 1.3 cm. Thus, based on the limited information available, it is unlikely that the orientations of the observed χ vectors for the BL Lacertae objects are appreciably affected by Faraday rotation.

Models for the VLBI source structures were derived by fitting the complex I and P visibilities that come from the hybrid mapping process as described by Roberts, Gabuzda & Wardle

 $^{^{1}}P=p\,\mathrm{e}^{2i\chi}=mI\,\mathrm{e}^{2i\chi},$ where p=mI is the polarized intensity, m is the fractional linear polarization, and χ is the position angle of the electric vector on the sky.

Table 2. VLBI source models.

	I (mJy)	p (mJy)	χ (deg)	m (%)	r (mas)	Δr (mas)	θ (deg)	$\Delta \theta$ (deg)	MAJ (mas)	MIN	PA
					0235	+164					
C	451	5.0	36	1.1	-	_	_	_	0.13		
					0300	+470					
C	371	7.8	-35	2.1	-	-	-	_	0.07		
K3	253	8.3	5	3.3	0.199	0.004	138.1	1.1	0.17		
K2	15	<4	_	<27	1.151	0.043	154.1	2.3	0.16		
K1	29	<4	_	<14	1.776	0.033	155.0	1.2	0.40		
	165	22.2	20	5.0		+178			0.00		
C	465	23.2	20	5.0	- 0.100	-	102.5	_	0.02		
K2	104 383	17.3	-66	16.6 <2	0.199	0.006	102.5 77.4	2.3	0.10 0.30		
K1	383	<6	_	<2	0.745	0.004 + 658	//.4	0.3	0.30		
С	375	10.2	-29	2.7	- 0934	-	_	_	0.00		
K3	34	5.3	11	15.6	0.289	0.011	-23.9	2.3	0.08		
K2	25	<3	_	<12	0.568	0.016	-17.5	1.3	0.11		
K1	24	<3	_	<12	1.002	0.042	-17.6	3.0	0.40		
		-				279					
C	6496	290	107	4.5	_	_	_	_	0.06		
K4	1681	341	53	20.3	0.120	0.005	-105.0	3.0	0.11		
K3	799	184	26	23.0	0.636	0.008	-131.2	0.8	0.10		
K2	177	<38	_	<21	0.835	0.025	-123.3	2.1	0.03		
K1c	240	<38	_	<16	2.351	0.031	-118.4	0.9	0.28		
K1b	162	52	46	32.1	2.769	0.039	-120.0	1.0	0.16		
K1a	830	105	89	12.6	2.713	0.007	-113.4	0.3	0.26		
						+784					
C	1396	51.6	17	3.7	-	-	_	-	0.09		
K3	148	<9	-	<6	0.194	0.005	-101.6	1.8	0.26		
K2	61	<9	_	<15	0.673	0.020	-94.3	1.7	0.52	0.22	2.1
K1	147	<9	-	<6	1.479	0.005 + 568	-95.4	0.3	0.56	0.32	31
C	1254	97.9	20	7.8	-	-	_	_	0.03		
K4	280	27.8	35	9.9	0.168	0.003	-163.7	1.0	0.07		
K3	96	12.0	34	12.5	0.430	0.004	-157.0	0.6	0.08		
K2	18	3.3	21	18.3	0.797	0.041	-152.4	1.9	0.31		
K1	18	<3	_	<17	1.762	0.050	-156.2	0.9	0.49	0.17	-155
					BL	Lac					
C	910	<6	_	< 0.6	-	_	_	_	0.07		
K5	422	24.5	19	5.8	0.288	0.004	-169.4	0.9	0.12		
K4	147	50.0	-15	34.0	0.782	0.014	-173.8	0.5	0.17		
K3	720	45.4	-9	6.3	1.285	0.006	-179.0	0.2	0.42		
K2	153	38.1	-60	24.9	1.419	0.014	-175.1	0.5	0.18		
K1	419	42.2	88	10.1	1.942	0.016	-164.9	0.5	0.81		

(1987) and Gabuzda, Wardle & Roberts (1989a). The columns in Table 2 give (1) the component's designation; (2)–(5) its total flux, polarized flux, polarization position angle, and degree of polarization; (6)–(7) its separation from the core and the uncertainty in this separation; (8)–(9) its structural position angle and the uncertainty in this angle, and (10)–(12) the major axis, minor axis, and position angle of the circular or elliptical Gaussian used to describe the component. The errors indicated are the formal 1σ errors corresponding to an increase of the minimum χ^2 by unity. The smallest of these almost certainly underestimate the true errors; realistically, the smallest 1σ errors in component separations are probably no less than ≈ 0.01 –0.02 mas.

We assume throughout a Friedmann universe with Hubble constant of $100\,h\,\mathrm{km\,s}^{-1}\,\mathrm{Mpc}^{-1}$ and $q_0=0.5$.

3.1 0235+164

0235+164 was first identified as a BL Lacertae object by Spinrad & Smith (1975). Emission lines at redshift $z_{\rm e} \simeq 0.94$ have been observed (Cohen, Smith & Burbidge 1986), making this one of the highest redshift BL Lacertae objects. There is an optical extension

about 3 arcsec to the south which displays absorption and emission lines at a redshift of 0.525 (Smith, Burbidge & Junkkarinen 1977); presumably this is the nucleus of an active galaxy that lies along the line of sight to the BL Lacertae object. The presence of this intervening galaxy and the extreme variability of 0235+164 led Stickel, Fried & Kuhr (1989) to suggest that this object could actually be a quasar that is being microlensed by stars in a foreground galaxy. The radio emission is unresolved on arcsecond scales (Kollgaard et al. 1992). There has been some evidence for weak extentions to the north-west on some VLBI maps (Bååth et al. 1981; Bååth 1984; Jones et al. 1984), but the position angles in which this structure lies vary significantly from epoch to epoch, and it is not clear that they represent a reliable detection of parsecscale structure. The 5- and 8-GHz VLBI images of Gabuzda et al. (1989b, 1992) and Gabuzda & Cawthorne (1996) did not reveal any structure.

Our 1.3-cm images (Fig. 1) show the source to be appreciably resolved, but no structural position angle is distinguished. We have fitted the observed visibility data with a single circular Gaussian component. This component is modestly polarized, m=1 per cent.

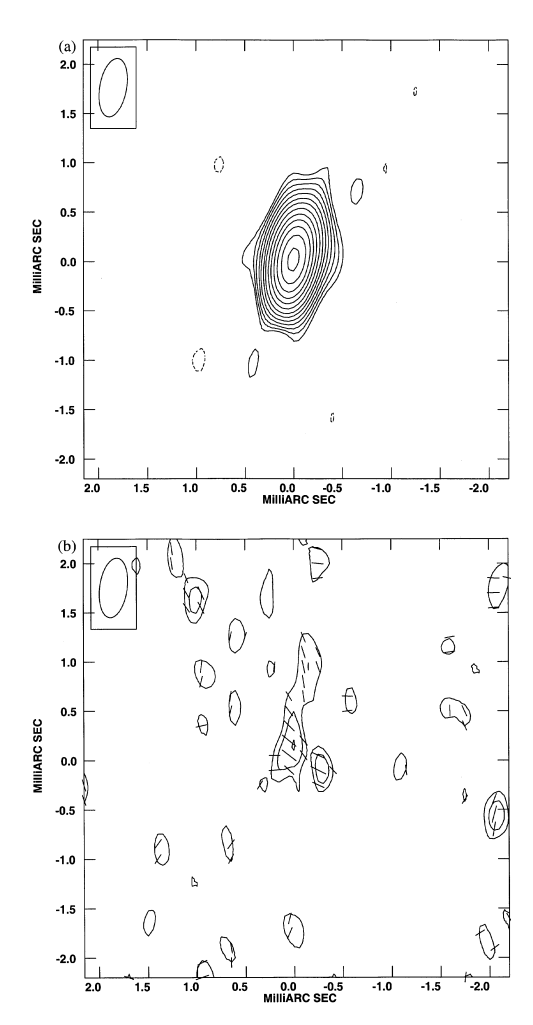


Figure 1. VLBI maps of 0235+164 at 1.3 cm, epoch 1995.58: (a) *I*, with contours at -1.4, 1.4, 2.0, 2.8, 4.0, 5.6, 8.0, 11.3, 16.0, 22.6, 32.0, 45.2, 64.0, and 90 per cent of the peak brightness of 0.40 Jy beam⁻¹. (b) *P*, with contours of polarized intensity at 48.0, 68.0, and 96.0 per cent of the peak brightness of 6.7 mJy beam⁻¹, and χ vectors superimposed.

3.2 0300+470

The redshift for 0300+470 is unknown. $\lambda20\,\mathrm{cm}$ and $\lambda6\,\mathrm{cm}$ VLA images made by Antonucci & Ulvestad (1985) and Kollgaard et al. (1992) have shown this source to have weak, one-sided emission extending roughly south of the VLA core. Previous VLBI images at 5 GHz (Gabuzda et al. 1992, 1994b) initially revealed a jet toward the east, but subsequently jet components were observed to emerge toward the south-east. It is not clear if jet features initially emerge in position angle $\approx135^\circ$ and then move north-eastward to join an eastern flow, or if the core has ejected jet components in different directions at different epochs.

The jet extending toward the south-east is clearly visible in our 1.3-cm image (Fig. 2). The jet shows some possible small wiggles, but there is no indication that it bends toward the north on the scales sampled by our VLB array. We modelled this structure as two bright components and two weaker components; polarization was detected in each of the bright components (the core and the inner jet). Fig. 2(c) shows that the polarization angle χ in the core is well aligned with the direction of the inner jet; the core is modestly polarized, m=2 per cent. The relationship between χ

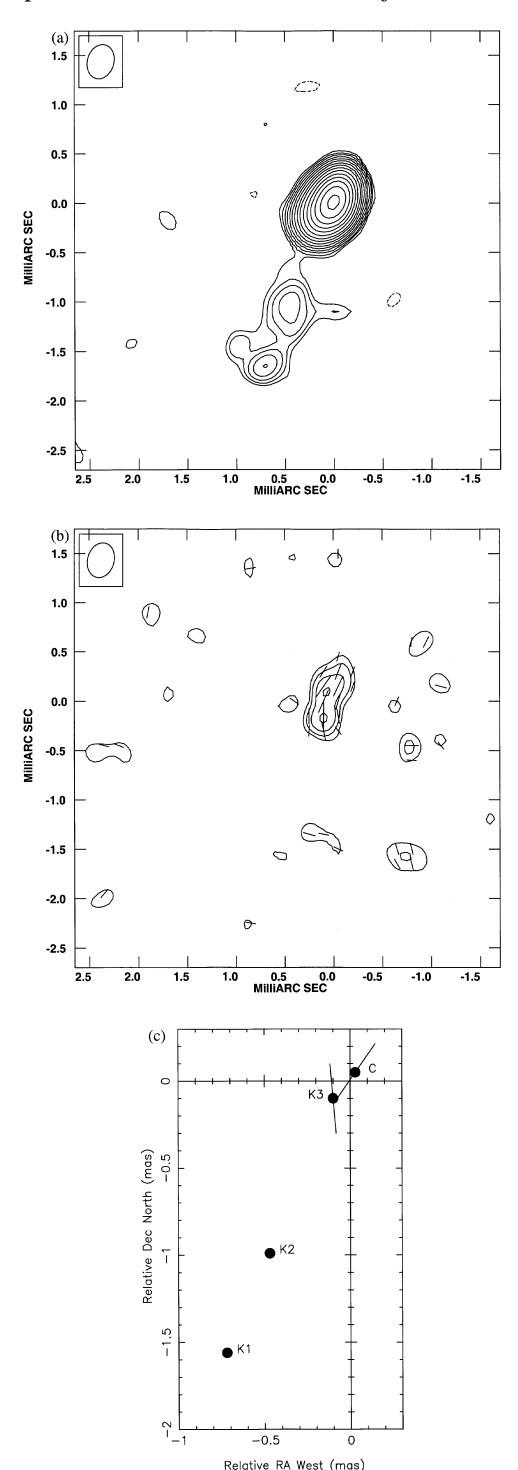


Figure 2. VLBI maps of 0300+470 at 1.3 cm, epoch 1995.58: (a) I, with contours at -0.7, 0.7, 1.0, 1.4, 2.0, 2.8, 4.0, 5.6, 8.0, 11.3, 16.0, 22.6, 32.0, 45.2, 64.0, and 90 per cent of the peak brightness of 0.46 Jy beam⁻¹. (b) P, with contours of polarized intensity at 34.0, 48.0, 68.0, and 96.0 per cent of the peak brightness of 9.0 mJy beam⁻¹, and χ vectors superimposed. (c) Plot of relative positions of model-fit components with χ vectors superimposed.

for the inner-jet component and the local jet direction is not clear: it is 47° from the direction back toward the core (i.e., upstream), and 28° from the direction toward the next further jet knot (i.e., downstream).

3.3 0735+178

0735+178 was first identified as a BL Lacertae object by Carswell et al. (1974); the optical spectrum is featureless except for two sharp absorption lines that have been identified with the Mg II λ 2798-Å doublet at a redshift of $z_a=0.424$. Observations by O'Dea, Barvainis & Challis (1988) show a slightly curved radio jet extending \approx 2 arcsec toward the south. The VLBI jet of 0735+178 extends toward the north-east, and has several superluminal components having apparent speeds $\beta_{\rm app}h \approx 4-7$ (Bååth & Zhang 1991; Gabuzda et al. 1994a, and references therein).

Our 1.3-cm image (Fig. 3) clearly shows the jet extending toward the east. The data are well fitted by a model with three circular Gaussian components – a core and two jet components, the second of which (at a distance of 0.75 mas from the core) is quite extended. Polarization was detected from the core and inner jet; there is some indication of polarization associated with the outer region of the extended outer jet component, but it is difficult to be sure whether or not this is a real detection. Fig. 3(c) shows the relative positions of the three model components and their χ s. The core is 5 per cent polarized, with χ nearly perpendicular to the direction toward the inner jet knot; the inner jet is more highly polarized ($m \approx 17$ per cent), with χ nearly parallel to the direction back toward the core.

3.4 0954+658

The redshift of 0954+658 is z=0.386 (Lawrence et al. 1986). VLA images by Perley (1982) and Kollgaard et al. (1992) have revealed a jet extending toward the south-west and then curving south, ending in a secondary component \simeq 4 arcsec from the VLA core. 5- and 8-GHz VLBI images show a very compact jet that initially emerges in structural position angle -30° and then curves toward the south-west (Gabuzda et al. 1992, 1994b); two superluminal components with apparent speeds $\beta_{\rm app}h=6.2$ and 5.2 have been identified.

Our 1.3-cm images (Fig. 4) clearly show for the first time the inner jet extending almost directly north, before it turns westward. The source structure is well described by a model with the core and three jet components. Polarization is detected from the core and innermost jet knot. As we can see in Table 2 and Fig. 4(c), the core is 2.7 per cent polarized, with χ well aligned with the direction toward the innermost knot (to within 5°). Although χ in the innermost knot does not bear any clear relation to the direction back toward the core, it is aligned with the direction downstream to the next knot to within $\approx 20^{\circ}$.

3.5 3C 279

3C 279 has a redshift z=0.538 (Burbidge & Rosenberg 1965; Lynds, Stockton & Livingston 1965). With respect to its VLBI properties, it is a somewhat unusual source: it is classified as an OVV quasar, but appears to exhibit some properties more characteristic of BL Lac objects. For example, the components in its VLBI jet, which lies at $\theta \simeq -120^\circ$, exhibit relatively 'slow' superluminal speeds (Unwin et al. 1989). In addition, there is evidence from integrated centimetre-wavelength monitoring data (Aller et al. 1985; Hughes, Aller & Aller 1989) that relativistic shocks dominate the integrated emission in at least some highly polarized radio outbursts; as noted above, symptoms of shocks are

often evident in the VLBI jets of BL Lacertae objects, but are less apparent in quasars.

Our 1.3-cm images (Fig. 5) show the VLBI jet and its rich polarization structure. There is a pronounced gap in the jet emission from about 0.85 mas to about 2.5 mas from the core. We

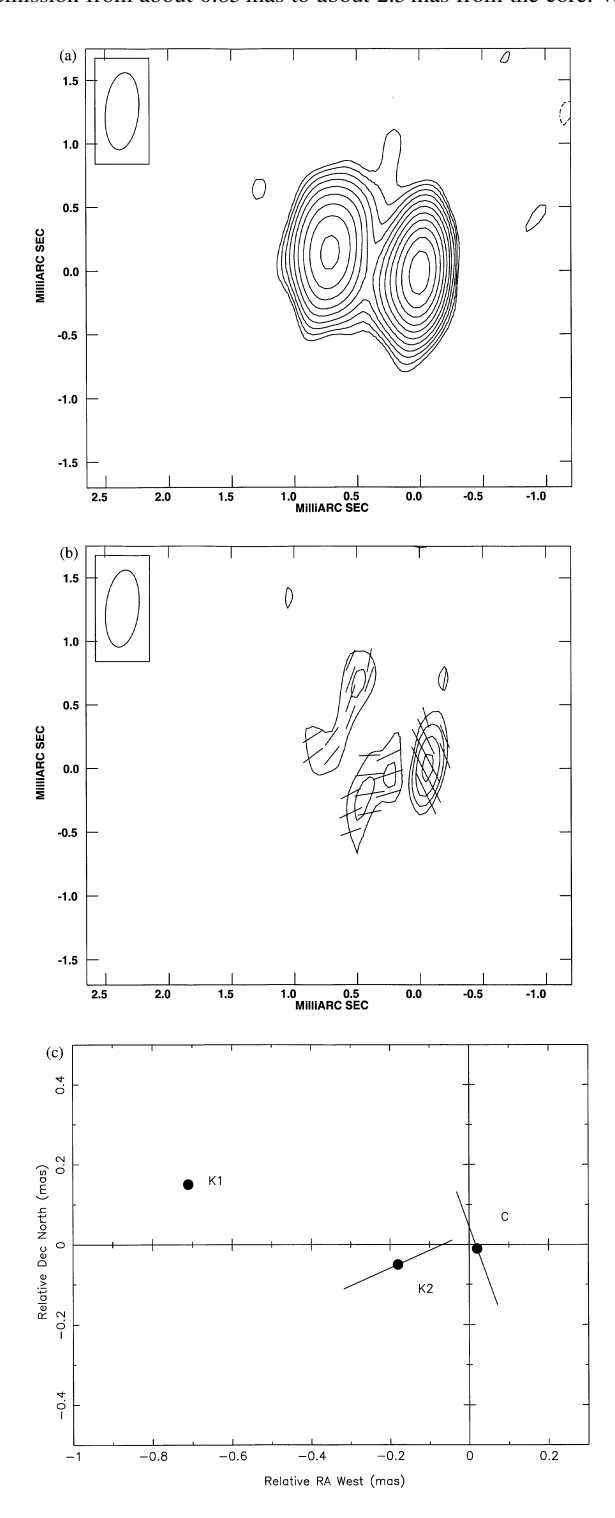


Figure 3. VLBI maps of 0735+178 at 1.3 cm, epoch 1995.58: (a) *I*, with contours at -2.5, 2.5, 3.5, 5.0, 7.0, 10.0, 14.0, 20.0, 28.0, 40.0, 56.0, and 80 per cent of the peak brightness of 0.49 Jy beam⁻¹. (b) *P*, with contours of polarized intensity at 34.0, 48.0, 68.0, and 96.0 per cent of the peak brightness of 16.8 mJy beam⁻¹, and χ vectors superimposed. (c) Plot of relative positions of model-fit components with χ vectors superimposed.

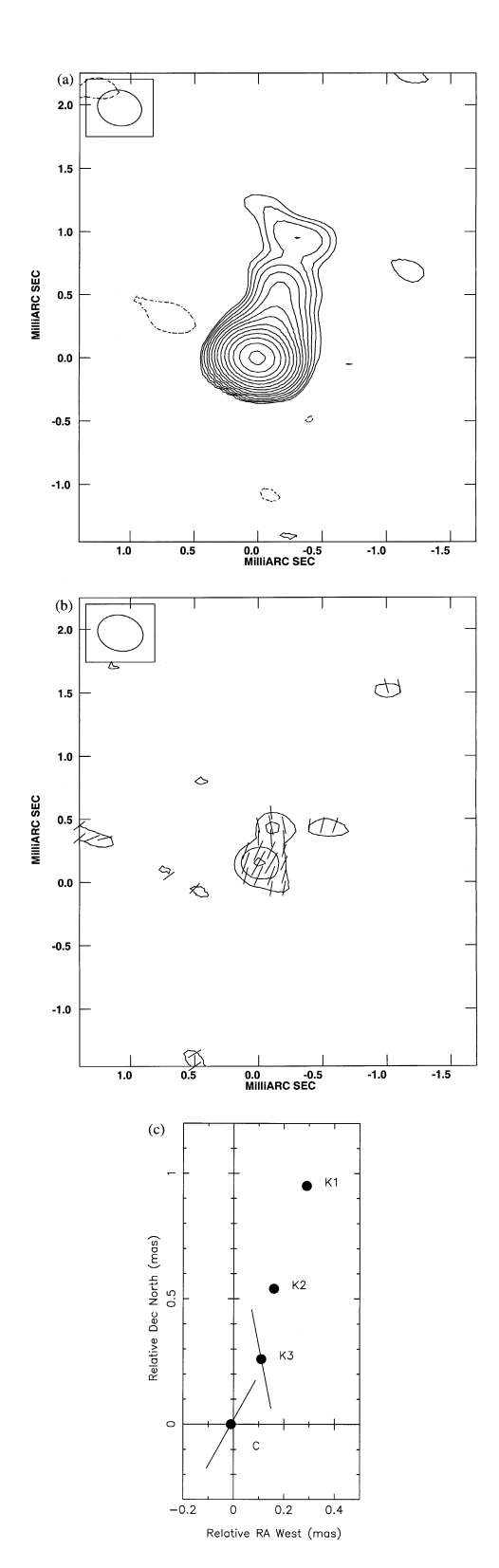


Figure 4. VLBI maps of 0954+658 at 1.3 cm, epoch 1995.58: (a) *I*, with contours at -1.0, 1.0, 1.4, 2.0, 2.8, 4.0, 5.6, 8.0, 11.3, 16.0, 22.6, 32.0, 45.2, 64.0, and 90 per cent of the peak brightness of 0.38 Jy beam⁻¹. (b) *P*, with contours of polarized intensity at 48.0, 68.0, and 96.0 per cent of the peak brightness of 7.2 mJy beam⁻¹, and χ vectors superimposed. (c) Plot of relative positions of model-fit components with χ vectors superimposed.

detected polarization in all but two of the jet components – the two nearest to this gap on either side; the remaining jet features are substantially polarized, ≈ 20 per cent. The core is moderately polarized, m = 4.5 per cent. Fig. 5(c) shows the relative positions

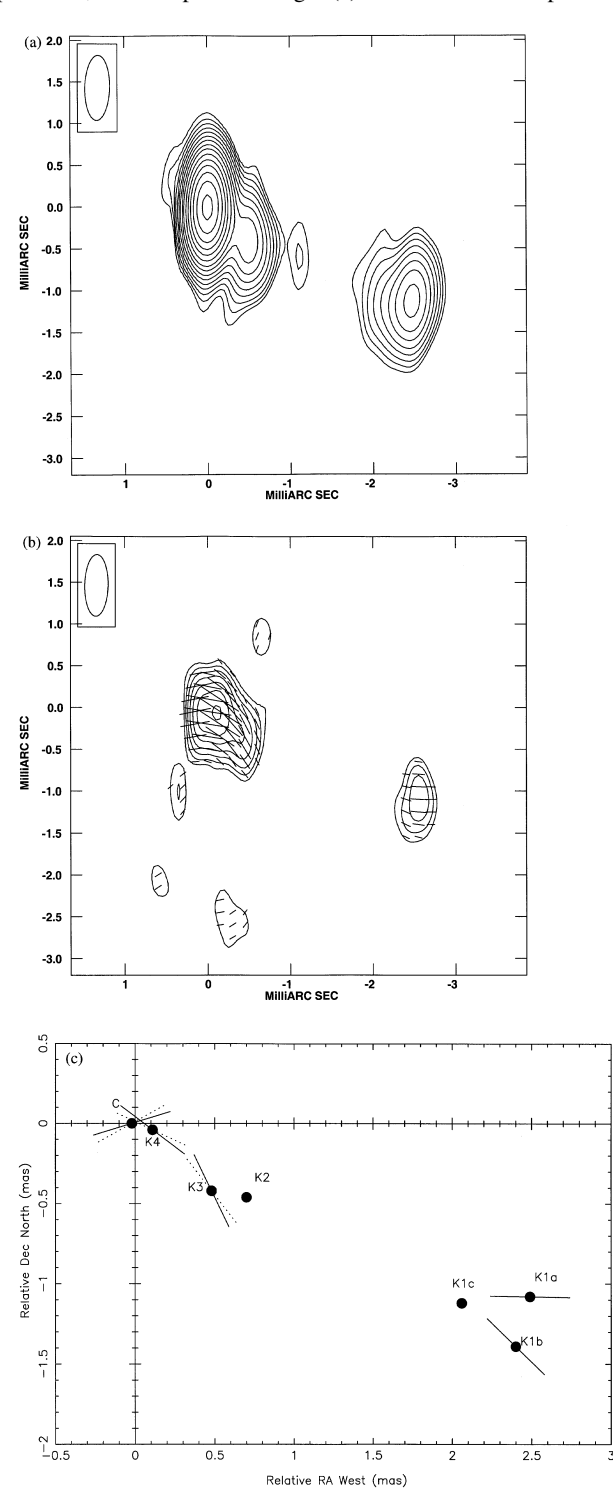


Figure 5. VLBI maps of 3C 279 at 1.3 cm, epoch 1995.58: (a) *I*, with contours at -0.7, 0.7, 1.0, 1.4, 2.0, 2.8, 4.0, 5.6, 8.0, 11.3, 16.0, 22.6, 32.0, 45.2, 64.0, and 90 per cent of the peak brightness of 7.44 Jy beam⁻¹. (b) *P*, with contours of polarized intensity at 12.0, 17.0, 24.0, 34.0, 48.0, 68.0, and 96.0 per cent of the peak brightness of 315.4 mJy beam⁻¹, and χ vectors superimposed. (c) Plot of relative positions of model-fit components with χ vectors superimposed.

of the *I* components with the observed χ vectors superimposed. We can see from this figure and the *P* map that the χ vectors for the jet emission between the core and the gap are aligned with the jet direction to within about 20° .

The 2–6 cm VLBA observations of Taylor (1998) indicated that, while the rotation measure of 3C 279 was quite small well out in the jet (more than about 1 mas from the core; $-64 \,\mathrm{rad}\,\mathrm{m}^{-2}$), the rotation measure in the core region was greatly enhanced, and equal to $-1280 \,\mathrm{rad}\,\mathrm{m}^{-2}$. This rotation measure implies a rotation of $+12^{\circ}$ at 1.3 cm. It therefore seems likely that some or all of our observed χ values for the core, K4, and K3 have been significantly affected by Faraday rotation. Unfortunately, the resolution of the images of Taylor (1998) is not sufficient to enable us to determine the appropriate corrections for the core, K4, and K3 separately.

If the rotation measure for all three of these components is close to $-1280\,\mathrm{rad\,m^{-2}}$, the derotated values χ_0 for the core, K4, and K3 are 119° , 65° and 38° , respectively. This brings χ for K3 into closer alignment with the direction upstream towards K4 (from 17° to 5°); it increases the offset between χ for K4 and the direction downstream toward K3 (from 10° to 22°), but decreases the offset between χ for K4 and the direction toward the core (from 22° to 10°). Thus, applying corrections for the core-region rotation measure determined by Taylor (1998) to the observed χ values for K3 and K4 does not change their general behaviour, but does decrease the maximum misalignment with the local jet direction to about 10° ; i.e., there is an overall improvement in the inferred alignment of χ_0 and the local jet direction. This provides circumstantial evidence that the rotation measures of these two components may, in fact, be close to the value of Taylor (1998).

The observed χ for the core (107° or -73°) is only poorly aligned with the direction toward the innermost jet feature ($\theta=-105^\circ$). Correcting for a rotation measure of $-1280\,\mathrm{rad}\,\mathrm{m}^{-2}$ moves the core χ away from this possible weak alignment, leaving its orientation relative to the inner jet arbitrary (an offset of 44°). This could represent genuine obliquity of the core magnetic field structure, although it is also possible that this reflects the direction of the jet flow on smaller scales, or that the rotation measure of the 1.3-cm core is significantly different from the value of Taylor (1998) for the 2-cm core. It is likely that there are rotation-measure gradients on the scales probed in our 1.3-cm images, so that the true rotation measures for the core, K4, and K3 probably differ somewhat from each other and from the value derived by Taylor for the 2-cm VLBI core region.

The set of three subcomponents K1a, K1b and K1c describing the outer jet requires a separate discussion. Here, the effect of the rotation measure is negligible at 1.3 cm. As shown in Fig. 5(c), we detected polarization in the two features K1a and K1b, which are at nearly the same distance from the core in somewhat different position angles. The interesting thing is that, in both of these features, χ is oriented back toward K1c. The east—west extension corresponding to K1a and K1c can clearly be seen in the total intensity image; χ in K1a is well aligned with this extension. At the same time, χ in K1b is much more similar to χ in the other jet features. This suggests that, indeed, the extended component about 2.5 mas from the core is complex, and may include separate regions with different flow directions.

3.6 1803+784

1803+784 has a redshift z=0.68 (Witzel et al. 1988). Arcsecond-scale radio images by Antonucci et al. (1986), Strom & Biermann (1991) and Kollgaard et al. (1992) show emission extending

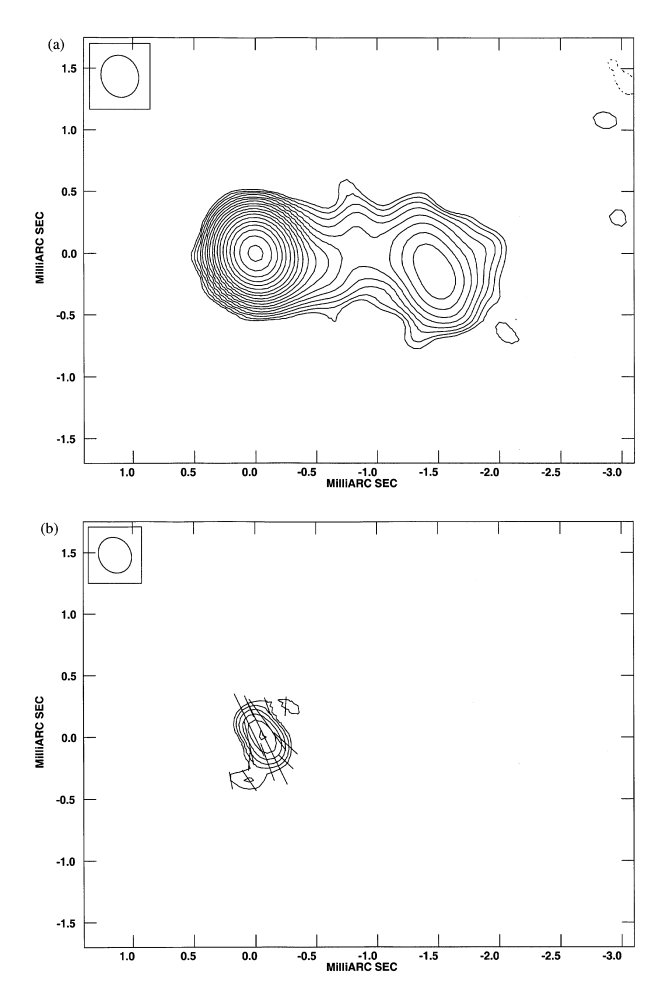


Figure 6. VLBI maps of 1803+784 at 1.3 cm, epoch 1995.58: (a) *I*, with contours at -0.25, 0.25, 0.25, 0.25, 0.5, 0.7, 1.0, 1.4, 2.0, 2.8, 4.0, 5.6, 8.0, 11.3, 16.0, 22.6, 32.0, 45.2, 64.0, and 90 per cent of the peak brightness of 1.35 Jy beam⁻¹. (b) *P*, with contours of polarized intensity at 17.0, 24.0, 34.0, 48.0, 68.0, and 96.0 per cent of the peak brightness of 52.6 mJy beam⁻¹, and χ vectors superimposed.

=2 arcsec to the south-west of the core, a weak secondary component =45 arcsec south and slightly west of the core, and a faint bridge of emission connecting the two. The VLBI jet of this source extends nearly directly west (Witzel et al. 1988; Gabuzda et al. 1992, 1994b). One VLBI component has been stationary over a period of more than 10 years; superluminal motion in another component with apparent speed $\beta_{app}h = 1.8$ has recently been detected (Gabuzda et al. 1994b). 6-cm space VLBI polarization observations of 1803 + 784 with *VSOP* show that its VLBI jet initially emerges to the north-west, then curves toward the south-west, with the magnetic field transverse all along the curved jet (Gabuzda 1999).

In the image presented here (Fig. 6), we can see the stationary feature ≈ 1.5 mas from the core. This feature is clearly extended along position angle $\approx 45^{\circ}$, in agreement with the 6-cm VSOP images (Gabuzda 1999). Unfortunately, no polarization was detected in the jet. The core is 3.7 per cent polarized; χ bears no obvious relation to the direction of the innermost jet component detected here. However, it is interesting that the core χ is perpendicular to the direction of the small-scale jet indicated by the 6-cm VSOP images (Gabuzda 1999) and the 3.6-cm images of Gabuzda & Cawthorne (1996). The absence of inner-jet

structure extending along a position angle of about -70° suggests that the jet ejection direction may have changed during the interval from the earlier 3.6-m observations of Gabuzda & Cawthorne (1996; epoch 1990.47) to our 1.3-cm observations

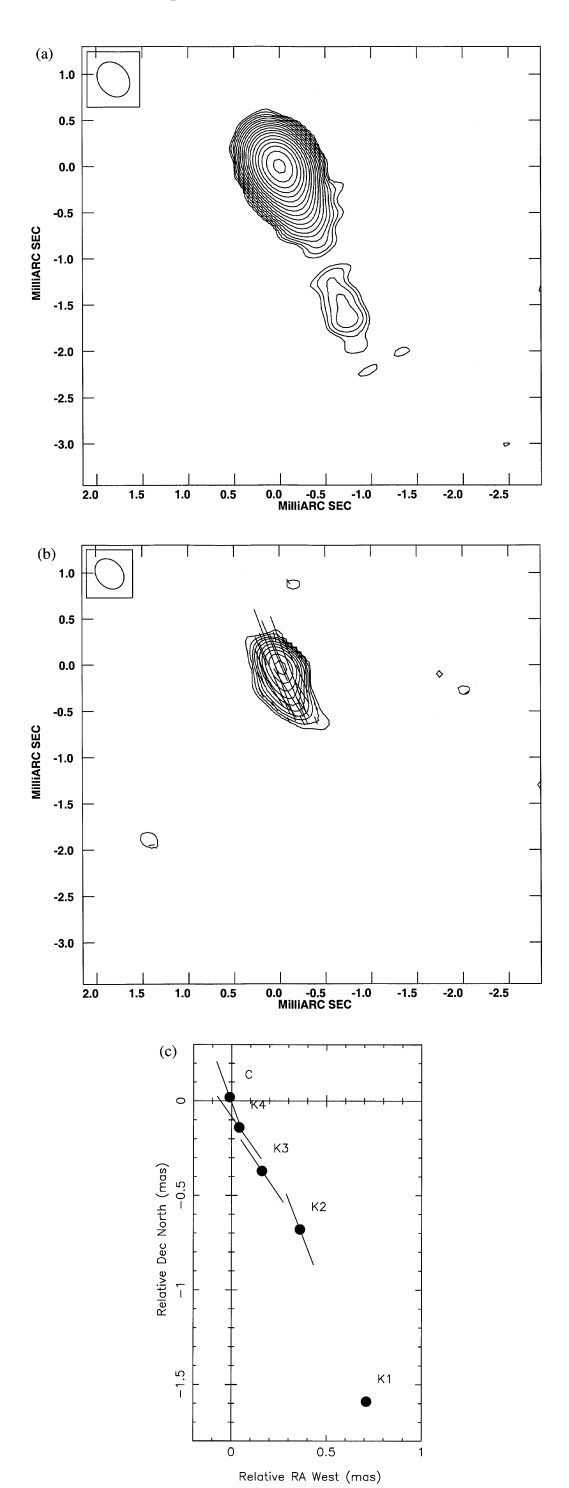


Figure 7. VLBI maps of 1823+568 at 1.3 cm, epoch 1995.58: (a) I, with contours at -0.25, 0.25, 0.25, 0.5, 0.5, 0.7, 1.0, 1.4, 2.0, 2.8, 4.0, 5.6, 8.0, 11.3, 16.0, 22.6, 32.0, 45.2, 64.0, and 90 per cent of the peak brightness of 1.44 Jy beam⁻¹. (b) P, with contours of polarized intensity at 4.0, 5.6, 8.0, 11.3, 16.0, 22.6, 32.0, 45.2, 64.0, and 90 per cent of the peak brightness of 109.6 mJy beam⁻¹, and χ vectors superimposed. (c) Plot of relative positions of model-fit components with χ vectors superimposed.

(1995.58). However, the orientation of the 1.3-cm core χ is consistent with the presence of motion in the core in position angle $\simeq -70^{\circ}$ on scales unresolved by our VLB array, suggesting that the jet-ejection direction has returned to its former value. This is consistent with the later (1998.55) 6-cm *VSOP* images, which clearly show the inner jet on submilliarcsecond scales to lie in position angle $\simeq -65^{\circ}$ (Gabuzda 1999). Thus the collected VLBI images for 1803+784 indicate possible time variability in the jet-ejection direction for this source.

3.7 1823+568

Lawrence et al. (1986) have assigned a tentative redshift of $z_{\rm e}=0.664$ to 1823+568. VLA observations at 5 GHz show a prominent jet extending toward the east (O'Dea, Barvainis & Challis 1988; Kollgaard et al. 1992). The VLBI jet extends slightly west of south (Pearson & Readhead 1988; Gabuzda et al. 1989, 1994b). Two superluminal components with apparent speeds $\beta_{\rm app}h \simeq 4$ have been identified (Gabuzda et al. 1994b).

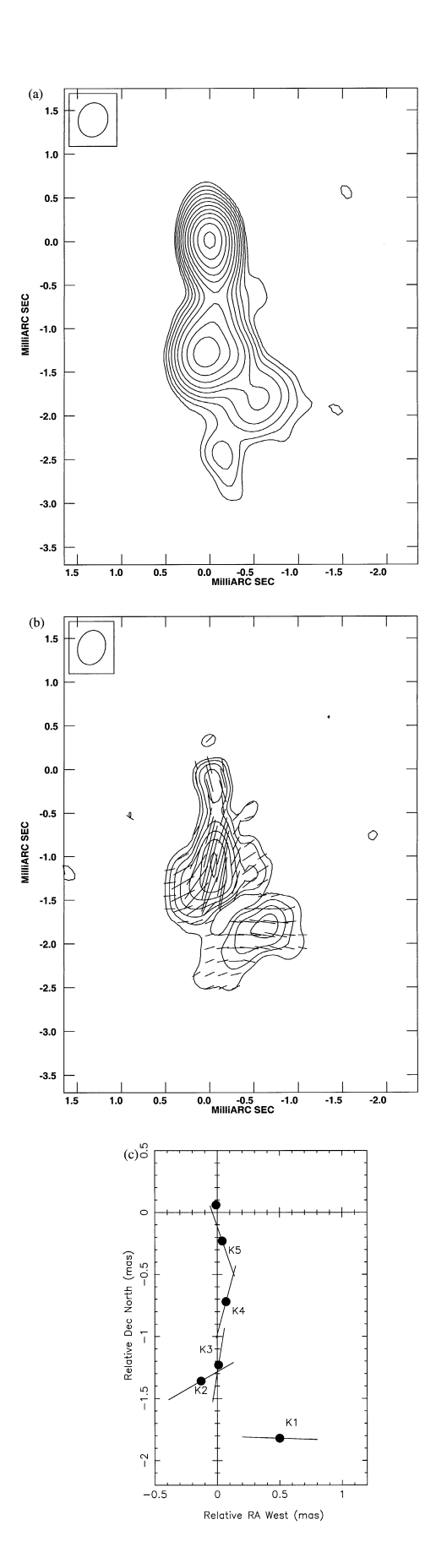
The VLBI jet extending to the south-west is clearly visible in Fig. 7. We modelled the I structure as a core with four jet components; we detected polarization in all components except for the outermost knot. Fig. 7(c) shows the relative positions of the I components with their χ values. The core χ is well aligned with the direction toward the innermost jet component K4. The χ s for the jet knots K4 and K3 are aligned with the direction downstream to within less than 10° , and χ for K2 is oriented very close to the direction toward the outermost knot K1. Thus, χ is aligned with our best estimate of the local jet direction along the entire detected VLBI structure. The core is relatively highly polarized, with $m \approx 8$ per cent, and the degrees of polarization in the jet are appreciable, $\approx 10-20$ per cent.

3.8 BL Lac

BL Lac lies at the centre of a giant elliptical galaxy; weak emission lines at a redshift $z_{\rm e}=0.069$ were detected by Miller, French & Hawley (1978). VLA maps by Antonucci et al. (1986) and Kollgaard et al. (1992) reveal the source to be very compact; the only arcsecond-scale structure is an extended halo-like structure with angular extent \approx 40 arcmin. The VLBI jet extends slightly west of south, then turns toward the east; Mutel et al. (1990) detected superluminal motion with apparent speeds $\beta_{\rm app}h\approx3.5$ in several VLBI components.

In the image in Fig. 8, the jet structure is complex. Our model fitting shows that most of the 1.3-cm emission can be described by a jet that initially emerges from the core in position angle $\theta \simeq -170^{\circ}$, then curves toward the east. This curvature is more clearly visible in Fig. 8(c), which shows the relative positions of the *I* components with their χ s superimposed. The χ s for K5, K4, K3, and K2 appear to be aligned with the local VLBI jet direction, and curve with the VLBI jet as it curves. The jet components are moderately to highly polarized, $m \simeq 6-34$ per cent, while the core is at best weakly polarized, m < 0.6 per cent.

The presence of the component K1 to the west of this main structure is a bit of a puzzle. Is this is a separate branch of the jet flow, or did K1 for some reason continue moving from the core in a relatively linear path rather than turning toward the east? It is also not clear what orientation the χ of K1 bears to the local flow direction.



4 DISCUSSION

4.1 Characteristics of the core polarizations

For the most part, the degrees of polarization of the 1.3-cm core components are similar to their characteristic values at 6 cm: $m \simeq 2-9$ per cent. It is interesting that, although the core polarization for 0954+658 (m=2.7 per cent) is within this typical range, this is substantially lower than values previously measured at 3.6 and 6 cm ($m \approx 10$ per cent). The core polarization for BL Lac (m < 0.6 per cent) is also lower than values measured at 6 cm. This type of behaviour was also shown in 3.6-cm VLBI polarization observations of nine BL Lacertae objects (Gabuzda & Cawthorne 1996), in which most of the core polarizations were similar to their usual 6-cm values, but several were appreciably lower. This is consistent with the idea that the cores of BL Lacertae objects are relatively strongly polarized at 6 cm because we are actually seeing a blend of emission from the intrinsically more weakly polarized core and highly polarized, optically thin emerging jet features (Gabuzda et al. 1994b). With the higher resolution provided by the 1.3-cm observations, we are able to better isolate the emission of the comparatively weakly polarized core. The maximum degree of polarization expected if the core components are optically thick is $m_{\text{core}} \approx 10 \text{ per cent}$ (Pacholczyk 1970). Thus the rather low polarizations observed for some objects $(m \le 1 \text{ per cent})$ cannot be explained as an optical depth effect alone, and appear to indicate the presence of tangled magnetic fields and/or depolarizing thermal plasma in the core region.

The χ values for the core components show a clear tendency to be either aligned with or perpendicular to the direction of the inner jet, as observed also for BL Lacertae objects at 3.6 and 6 cm (Gabuzda & Cawthorne 1996; Gabuzda et al. 2000) and six blazars at 7 mm (Lister, Marscher & Gear 1998). Among the BL Lacertae objects, the only possibly oblique core χ is that for 1803+784; however, here χ is perpendicular to the direction of the inner jet indicated by 6-cm space VLBI images (Gabuzda 1999) and 3.6-cm ground-based images at other epochs (Gabuzda & Cawthorne 1996), suggesting that the core χ reflects the direction of motion of imminently emerging new jet components.

In 0300+470 and 0735+178, the core χ values are respectively aligned with and perpendicular to the direction toward the innermost jet component to within less than 10° ; the alignments for 0954+658 and 1823+568 are to within 5° . This good alignment suggests that regions of enhanced rotation measure such as those detected by Taylor (1998) may not less common in BL Lacertae objects than in quasars. Multiwavelength VLBI polarization studies of BL Lacertae objects with as high resolution as possible are required to test this possibility.

4.2 Characteristics of the jet polarizations

The degrees of polarization of the jet components are also comparable to those observed at longer centimetre wavelengths. The χ s for jet components show a clear tendency to be aligned

Figure 8. VLBI maps of BL Lac at 1.3 cm, epoch 1995.58: (a) *I*, with contours at -2.0, 2.0, 2.8, 4.0, 5.6, 8.0, 11.3, 16.0, 22.6, 32.0, 45.2, 64.0, and 90 per cent of the peak brightness of 0.97 Jy beam⁻¹. (b) *P*, with contours of polarized intensity at 12.0, 17.0, 24.0, 34.0, 48.0, 68.0, and 96 per cent of the peak brightness of 51.1 mJy beam⁻¹, and χ vectors superimposed. (c) Plot of relative positions of model-fit components with χ vectors superimposed.

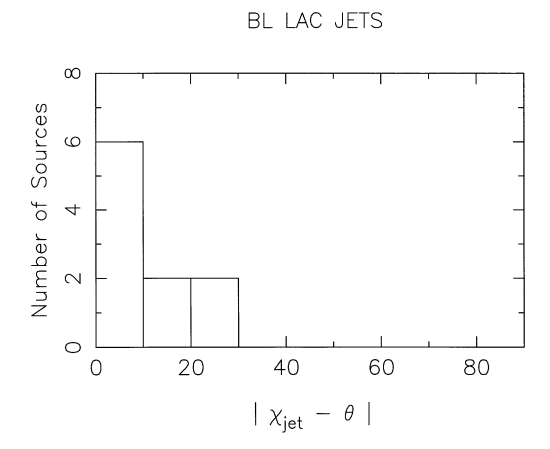


Figure 9. Histogram of the offset between polarization position angle and local jet direction $|\chi_{\rm jet} - \theta|$ for all BL Lacertae object jet components for which polarization was detected. The component K1 in BL Lac is not included, since we have no information about the local jet direction for this feature.

with the local jet direction, in some cases rotating to stay aligned with the jet as it bends (e.g., BL Lac). The only BL Lacertae object in which jet polarization was detected and the jet χ is *not* aligned with the local jet direction to within 20° or less is 0300+470 (K3, Fig. 2). In this source, χ in the jet feature K3 is 28° offset from the direction toward the next jet knot, K2 – an appreciably worse alignment than for the other BL Lacertae objects, particularly since the jet near K3 seems to be very straight.

Thus at least five of the six sources with detected jet polarization (including 3C 279), and possibly all six, have jet χ s aligned with the local jet direction (Fig. 9). This result stands in sharp contrast to the distribution of $|\chi_{\rm jet} - \theta|$ reported by Lister et al. (1998) for a group of about a dozen blazars, which was essentially uniform from 0°–90°. It is possible that Lister et al. (1998) were comparing $\chi_{\rm jet}$ with inaccurate inferred values for the local jet direction. More recent 43-GHz results for sources from a complete sample of radio-loud AGN including 10 BL Lacertae objects indicate a $|\chi_{\rm jet} - \theta|$ distribution similar to our 22-GHz distribution, with a high fraction of the jet χ s aligned with the jet direction (Lister et al. 2000).

VLBI polarization observations of a complete sample of radio-loud BL Lacertae objects at 6 cm (Gabuzda et al. 2000) have shown that, in fact, about 30 per cent of the sources have longitudinal magnetic fields in at least some parts of their VLBI jets. In contrast, we have seen no cases of longitudinal jet fields among the 1.3-cm polarization images considered here. However, early 6-cm VLBI polarization results also suggested that all VLBI jets in BL Lacertae objects had transverse magnetic fields, and it was only when more systematic studies of larger and more complete samples were done that it became clear that this was not the case. Thus it is too early to tell whether transverse magnetic field structures are more dominant in the jets of BL Lacertae objects on the smaller scales probed by 1.3-cm and 7-mm observations.

5 SUMMARY

We have presented 1.3-cm total intensity and linear polarization images for seven BL Lacertae objects and the OVV quasar 3C 279. On the whole, these images have shown similar

tendencies as those seen in 3.6- and 6-cm images with somewhat lower resolution. The overall properties of 3C 279 in our images are quite consistent with those for the BL Lacertae objects.

The core components are usually appreciably polarized, although there are several cases in which the core polarizations are lower than those observed at 6 cm. This is consistent with a picture in which the 6-cm core polarizations are often dominated by the contribution of highly polarized new knots – the higher resolution 1.3-cm observations better isolate the intrinsic core polarization. The core polarization position angles show a clear tendency to be either parallel to or perpendicular to the inner-jet direction, as is also observed at longer centimetre wavelengths.

The jet components are substantially polarized, at levels comparable to those observed at 3.6 and 6 cm, with χ aligned with the local jet direction in essentially all cases. The appreciable degrees of polarization of the jet emission indicate that it is optically thin, implying that the underlying magnetic fields are transverse. Such field structures have usually been interpreted as evidence that the visible jet components are associated with relativistic shocks that compress an initially tangled magnetic field, enhancing the magnetic field transverse to the compression (Laing 1980; Hughes et al. 1989). It also seems likely that, in at least some cases, we are seeing the dominant toroidal component of helical fields associated with the jet (Gabuzda 1999; Gabuzda et al. 2000).

The results presented here are reminiscent of those for early VLBI polarization images at 6 cm, which also suggested that the dominant fields in the jets of BL Lacertae objects were essentially always transverse. More thorough studies of complete samples of objects demonstrated that, in fact, a sizeable minority of BL Lacertae objects have 6-cm jet components with longitudinal fields. It remains to be seen if this will also be the case for the scales probed by 1.3-cm and 7-mm VLBI observations.

ACKNOWLEDGMENTS

DCG acknowledges support from the European Commission under TMR contract No. ERBFMGECT950012. TVC acknowledges support from UK PPARC. The National Radio Astronomy Observatory is operated by Associated Universities, Inc., under cooperative agreement with the NSF. This research has made use of data from the University of Michigan Radio Astronomy Observatory, which is supported by the National Science Foundation and by funds from the University of Michigan. Finally, we thank the anonymous referee for a careful review of the manuscript.

REFERENCES

Aller H. D., Aller M. F., Latimer G. E., Hodge P. E., 1985, ApJS, 59, 513 Angel J. R. P., Stockman H. S., 1980, ARA&A, 18, 321 Antonucci R. R. J., Ulvestad J. S., 1985, ApJ, 294, 158

Antonucci R. R. J., Hickson P., Olszewski E. W., Miller J. S., 1986, AJ, 92,

Bååth L. B., 1984, in Fanti R., Kellermann K., Setti G., eds, Proc. IAU Symp. 110, VLBI and Compact Radio Sources. Reidel, Dordrecht, p. 127

Bååth L. B., Zhang F. J., 1991, A&A, 243, 328

Bååth L. B., Elgered G., Lundqvist G., Graham D., Weiler K. W., Seielstad
G. A., Tallqvist S., Schilizzi R. T., 1981, A&A, 96, 316
Burbidge E. M., Rosenberg F. D., 1965, ApJ, 142, 1673

Carswell R. F., Strittmatter P. A., Williams R. D., Kinman T. D., Serkowski K., 1974, ApJ, 190, L101

- Cohen R. D., Smith H. E., Burbidge E. M., 1986, BAAS, 18, 674 Falomo R., 1996, MNRAS, 283, 241
- Gabuzda D. C., 1999, New Astron. Rev., 43, 691
- Gabuzda D. C., 2000, in Hirabayashi H., Edwards P. G., Murphy D. W., eds, Astrophysical Phenomena Revealed by Space VLBI. ISAS, Tokyo, p. 121
- Gabuzda D. C., Cawthorne T. V., 1996, MNRAS, 283, 759
- Gabuzda D. C., Wardle J. F. C., Roberts D. H., 1989a, ApJ, 338, 743
- Gabuzda D. C., Cawthorne T. V., Roberts D. H., Wardle J. F. C., 1989b, ApJ, 347, 701
- Gabuzda D. C., Cawthorne T. V., Roberts D. H., Wardle J. F. C., 1992, ApJ, 388, 40
- Gabuzda D. C., Wardle J. F. C., Roberts D. H., Aller M. F., Aller H. D., 1994a, ApJ, 435, 128
- Gabuzda D. C., Mullan C. M., Cawthorne T. V., Wardle J. F. C., Roberts D. H., 1994b, ApJ, 435, 140
- Gabuzda D. C., Pushkarev A. B., Cawthorne T. V., 1999, MNRAS, 307, 725
- Gabuzda D. C., Pushkarev A. B., Cawthorne T. V., 2000, MNRAS, in press Gabuzda D. C., Pushkarev A. B., Garnich N. N., 2001, MNRAS, submitted Hughes P. A., Aller H. D., Aller M. F., 1989, ApJ, 341, 68
- Jones D. L., Bååth L. B., Davis M. M., Unwin S. C., 1984, ApJ, 284, 60 Kollgaard R. I., 1994, Vistas Astron., 38, 29
- Kollgaard R. I., Roberts D. H., Wardle J. F. C., Gabuzda D. C., 1992, AJ, 104, 687
- Laing R., 1980, MNRAS, 193, 439
- Lawrence C. R., Pearson T. J., Readhead A. C. S., Unwin S. C., 1986, AJ, 91, 494

- Lister M. L., Marscher A. P., Gear W. K., 1998, ApJ, 504, 702
- Lister M. L., Preston R. A., Piner B. G., Tingay S. J., 2000, in Hirabayashi H., Edwards P. G., Murphy D. W., eds, Astrophysical Phenomena Revealed by Space VLBI. ISAS, Tokyo, p. 203
- Lynds C. R., Stockton A. N., Livingston W. C., 1965, ApJ, 142, 1667 Miller J. S., 1981, PASP, 93, 681
- Miller J. S., French H. B., Hawley S. A., 1978, in Wolfe A., ed., Pittsburgh Conference on BL Lac Objects. Univ. Pittsburgh, Pittsburg, p. 176
- Mutel R. L., Phillips R. B., Bumei Su X., Buccifero R. R., 1990, ApJ, 352, 81
- O'Dea C. P., Barvainis R., Challis P., 1988, AJ, 96, 435
- Pacholczyk A. G., 1970, Radio Astrophysics. Freeman, San Francisco
- Pearson T. J., Readhead A. C. S., 1988, ApJ, 328, 114
- Perley R. A., 1982, AJ, 87, 859
- Roberts D. H., Gabuzda D. C., Wardle J. F. C., 1987, ApJ, 323, 536
- Smith H. E., Burbidge E. M., Junkkarinen V. T., 1977, ApJ, 218, 611
- Spinrad H., Smith H. E., 1975, ApJ, 201, 275
- Stickel M., Fried J. W., Kühr H., 1989, A&AS, 80, 113
- Strom R. G., Biermann P. L., 1991, A&A, 242, 313
- Taylor G. B., 1998, ApJ, 506, 637
- Unwin S. C., Cohen M. H., Biretta J. A., Hodges M. W., Zensus J. A., 1989, ApJ, 340, 117
- Witzel A., Schalinski C. J., Johnston K. J., Biermann P. L., Krichbaum T. P., Hummel C. A., Eckart A., 1988, A&A, 206, 245

This paper has been typeset from a TEX/LATEX file prepared by the author.